JACS
JOURNAL OF THE AMERICAN CHEMICAL SOCIETY
Article
pubs.acs.org/JACS

Strong Photon Energy Dependence of the Photocatalytic Dissociation Rate of Methanol on TiO_2(110)

Chengbiao Xu,[†,⊥,∥] Wenshao Yang,[†,∥] Zefeng Ren,[§] Dongxu Dai,[†] Qing Guo,*[,†] Timothy K. Minton,*[,†,‡] and Xueming Yang*[,†]

[†]State Key Laboratory of Molecular Reaction Dynamics, Dalian Institute of Chemical Physics, Chinese Academy of Sciences, 457 Zhongshan Road, Dalian 116023, P. R. China

[‡]Department of Chemistry and Biochemistry, Montana State University, PO Box 173400, Bozeman, Montana 59717, United States

[§]International Center for Quantum Materials, Peking University, 5 Yiheyuan Road, Beijing 100871, P. R. China

Supporting Information

ABSTRACT: Photocatalytic dissociation of methanol (CH_3OH) on a TiO_2(110) surface has been studied by temperature programmed desorption (TPD) at 355 and 266 nm. Primary dissociation products, CH_2O and H atoms, have been detected. The dependence of the reactant and product TPD signals on irradiation time has been measured, allowing the photocatalytic reaction rate of CH_3OH at both wavelengths to be directly determined. The initial dissociation rate of CH_3OH at 266 nm is nearly 2 orders of magnitude faster than that at 355 nm, suggesting that CH_3OH photocatalysis is strongly dependent on photon energy. This experimental result raises doubt about the widely accepted photocatalysis model on TiO_2, which assumes that the excess potential energy of charge carriers is lost to the lattice via strong coupling with phonon modes by very fast thermalization and the reaction of the adsorbate is thus only dependent on the number of electron−hole pairs created by photoexcitation.

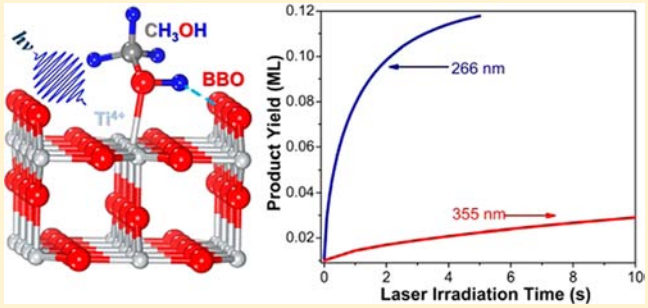

INTRODUCTION

Since the discovery of the photocatalytic splitting of water (H_2O) on TiO_2 electrodes by Fujishima and Honda in 1972,[1] tremendous research efforts have gone into understanding the fundamental processes and in enhancing the photocatalytic efficiency of TiO_2.[2] These efforts have been driven by the potential benefits to renewable energy, energy storage, and environmental cleanup.[3,4] In particular, TiO_2 has attracted much attention because of its applications in heterogeneous catalysis, photocatalysis, solar energy devices, etc.[5−14]

In an ideal photocatalyst, all photon energy invested in the generation of charge carriers would be available for redox chemistry. The higher the potential energy of the electron (or hole) the more reductive (or oxidative) capacity there is.[15] But charge carrier thermalization is rapid. For example, Gundlach and co-workers used two photon photoemission (2PPE) to track thermalization following electron injection from two dyes adsorbed on rutile TiO_2(110).[16,17] Fast initial decay of the 2PPE signal resulting from thermalization of the injected electron occurred on the 10 fs time scale. This result suggests that excess potential energy is lost to the lattice via strong coupling with phonon modes, thus reducing the potential advantage gained by the specificity in the absorption event. Additional evidence for the rapid thermalization of electrons comes from photoemission spectra of Ag clusters on rutile TiO_2(110)[18] as a function of injection electron energy and from photoluminescence spectra of rutile TiO_2(110)[19,20] with 3.35 eV photon irradiation. In both these studies, a constant energy of the emitted photons was observed (at and below the band gap energy—3.05 eV), independent of the energy of the exciting electron or photon. Furthermore, experimental investigations indicate that the photodesorption yield and translational energy of O_2 from an O_2-adsorbed TiO_2(110) surface are independent of the excitation photon energy above 3.4 eV, but instead depend on the photon flux.[21,22] It has also been reported that the photooxidation yield of hexane on a TiO_2 powder is dependent on photon flux rather than photon energy.[23] On the other hand, it has been reported that the photodesorption and photooxidation yields of other organics on TiO_2 are strongly dependent on photon energy.[24−26] Actually, the measurement of wavelength dependent yields of reaction products is not the best approach to understand the fundamental processes of photocatalysis. Instead of product yields, a wavelength-dependent rate measurement for a photocatalytic reaction system would be a more direct probe of the underlying mechanisms. We have thus investigated the wavelength dependence of the initial rate of the photocatalytic dissociation of methanol (CH_3OH) on TiO_2(110).

Received: November 10, 2013
Published: December 3, 2013

   dx.doi.org/10.1021/ja4114598 | J. Am. Chem. Soc. 2013, 135, 19039−19045

CH_3OH photocatalysis on $TiO_2(110)$ has become a well-studied model system and is thus an ideal testing ground for important photocatalysis concepts. Previous studies showed that molecular hydrogen production from H_2O on TiO_2 could be significantly enhanced by adding CH_3OH,[27] suggesting that CH_3OH plays an important role in photocatalytic H_2O splitting. Because of the importance of this issue, many experimental and theoretical studies have been carried out on the CH_3OH-$TiO_2(110)$ system.[28−39] In recent years, CH_3OH photochemistry on the rutile $TiO_2(110)$ surface has been investigated using various techniques, such as 2PPE, scanning tunneling microscopy (STM), and temperature programmed desorption (TPD), in order to understand CH_3OH photochemistry on $TiO_2(110)$ at the molecular level.[40−46] Using 2PPE and STM, Zhou et al.[40] concluded that photocatalytic dissociation of CH_3OH on $TiO_2(110)$ occurs at the Ti_{5c} adsorption sites. In a recent study,[44] we have shown that photocatalytic dissociation of CH_3OH on $TiO_2(110)$ occurs in a stepwise manner in which the O−H dissociation proceeds first and is then followed by C−H dissociation to form formaldehyde (CH_2O). Henderson and co-workers also observed the second step, photocatalytic C−H dissociation from CH_3O to form CH_2O.[45,46] Theoretical calculations for the ground electronic state show that the first step is nearly thermoneutral with a small barrier (0.25−0.3 eV),[31,36,43,44] suggesting that O−H bond dissociation is facile, while the second step has a much high barrier. By extending the detailed studies of CH_3OH photocatalysis on $TiO_2(110)$ to include wavelength-dependent rate measurements, we are able to go beyond the relatively simple description of the CH_3OH decomposition steps and their energetics and actually probe the fundamental process by which the photon energy initiates this decomposition.

EXPERIMENTAL DETAILS

Photocatalysis of CH_3OH was studied on a vacuum annealed $TiO_2(110)$ surface with a TPD apparatus[44,47] in combination with laser surface irradiation at 266 and 355 nm. The base pressure of the main chamber was 6×10^{-11} Torr. TPD products were detected with a quadrupole mass spectrometer (Extrel), which uses a specially designed electron-impact ionization region that can be maintained at an extremely high vacuum of 1.5×10^{-12} Torr. The rutile $TiO_2(110)$ crystal (Princeton Scientific Corp.) was cleaned through multiple cycles of Ar^+ sputtering and UHV annealing at 850 K until all surface contaminations were below the detection limit of Auger electron spectroscopy and a sharp (1 × 1) LEED pattern was observed. After this surface cleaning procedure, the crystal color became blue, and an oxygen vacancy population of about 4%, determined by H_2O TPD measurement,[48] was created on surface. Daily cleaning was accomplished by annealing the crystal at 850 K for 30 min in UHV. CH_3OH with a purity of >99.9% was purchased from Sigma-Aldrich. Before using, it was purified further by several freeze−pump−thaw cycles. In this experiment, we dosed the surface at 110 K with a 0.5 ML (1 ML = 5.2×10^{14} molecules cm^{-2}) coverage of CH_3OH using a home-built, calibrated, molecular beam doser.

The third harmonic (355 nm) or fourth harmonic (266 nm) output of a diode-pumped, solid state (DPSS), Q-switched 1064 nm laser (Spectra-Physics) was used to induce photochemistry on the CH_3OH adsorbate. The laser pulse duration was about 12 ns, and the laser repetition rate was 50 kHz. In order to minimize the temperature increase of the surface resulting from laser irradiation and to reduce surface damage by laser irradiation, only 40 mW of laser light at both wavelengths was used to illuminate the $TiO_2(110)$ surface. The laser beam diameter was 6 mm, and its incident angle was ∼30° with respect to the normal of the 10 × 10 mm^2 $TiO_2(110)$ surface, which was mounted with an angle point at the top (see Figure S1). The irradiated surface area was 56% of the total surface area. The laser flux was thus 9.5×10^{16} photons cm^{-2} s^{-1} for 266 nm and 1.3×10^{17} photons cm^{-2} s^{-1} for 355 nm. The TiO_2 surface temperature rose by about 5 K with the surface temperature at 110 K, and we found that the surface damage at both 355 and 266 nm was negligible during the exposure times used in our experiments (0−5 s at 266 nm and 0−600 s at 355 nm). These times were chosen such that CH_3OH dissociation to CH_3O and CH_2O were the dominant processes. Secondary processes, such as methyl formate ($HCOOCH_3$) formation from cross coupling reactions,[49] were observable but not significant. TPD measurements were carried out with a heating rate of 2 K/s. The $TiO_2(110)$ surface was annealed in vacuum at 850 K for 20 min between different TPD runs to maintain a flat and clean surface.

RESULTS

Figure 1A shows typical TPD spectra collected at a mass-to-charge ratio (m/z) of 31 for 0.5 ML of CH_3OH adsorbed on a

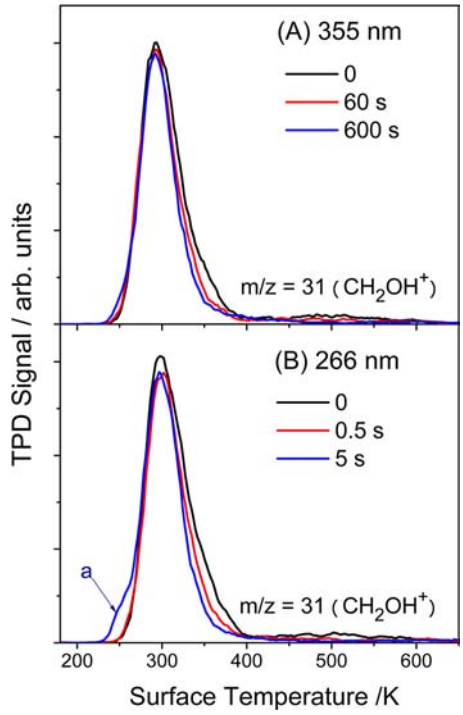

Figure 1. (A) Typical TPD spectra collected at m/z = 31 (CH_2OH^+) following different laser irradiation times at 355 nm. CH_2OH^+ is formed by dissociative ionization of the desorbed parent CH_3OH molecule in the electron-bombardment ionizer. (B) Typical TPD spectra collected at m/z = 31 following different laser irradiation times at 266 nm. Note "a" indicates the appearance of the methyl formate product at the longest irradiation times.[49] The broad peak near 500 K is attributed to recombinative desorption of some methoxy groups, resulting from dissociation at vacancy or nonvacancy sites.[42]

$TiO_2(110)$ surface, with different irradiation times (0−600 s), using 355 nm laser light. As the main feature at 300 K in the TPD spectra at m/z = 31 is exactly the same as that at m/z = 32 (not shown), this feature is assigned to desorption of molecularly adsorbed CH_3OH. A broad TPD peak around 500 K is also seen, and it is attributed to the recombinative desorption of dissociated CH_3OH on surface vacancy sites.[42] The TPD peak area for molecularly desorbed CH_3OH decreases by 16% after 600 s of 355 nm laser irradiation, suggesting that the CH_3OH molecules adsorbed on the five-coordinated Ti^{4+} (Ti_{5c}) sites were photocatalytically dissociated. This observation is consistent with our previous TPD

dx.doi.org/10.1021/ja4114598 | J. Am. Chem. Soc. 2013, 135, 19039−19045

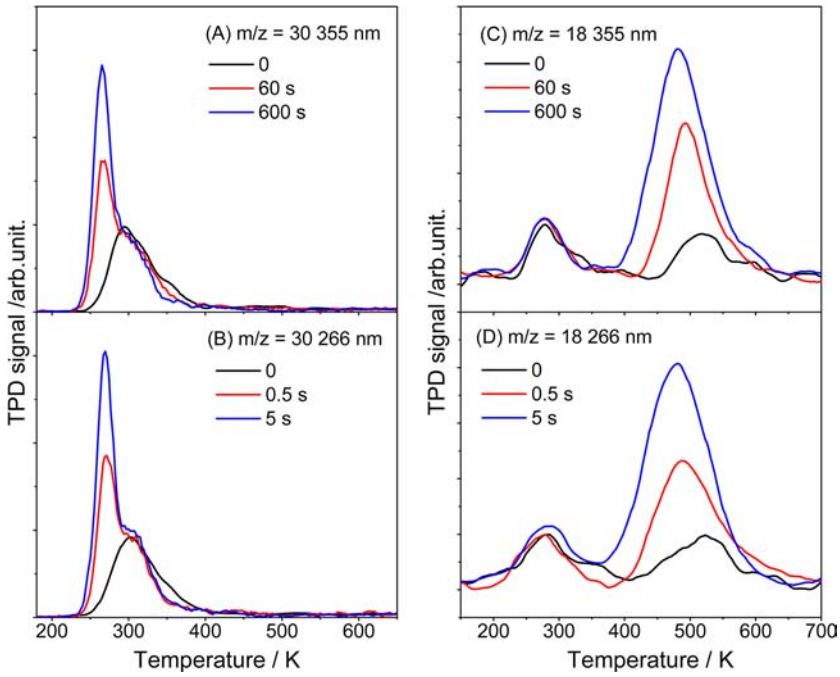

Figure 2. (A) TPD spectra collected at m/z = 30 (CH_2O^+) after laser irradiation times of 0, 60, and 600 s at 355 nm. (B) TPD spectra collected at m/z = 30 after laser irradiation times of 0, 0.5, and 5 s at 266 nm. (C) TPD spectra collected at m/z = 18 (H_2O^+) after laser irradiation times of 0, 60, and 600 s at 355 nm. The peak near 270 K arises from the small amount of H_2O impurity in the CH_3OH sample and the dissociative ionization signal of molecularly adsorbed CH_3OH in the electron-impact ionizer, while the peak near 500 K is the H_2O TPD product formed from recombination of two H-atoms and one O-atom on a BBO row. (D) TPD spectra collected at m/z = 18 after laser irradiation times of 0, 0.5, and 5 s at 266 nm.

results on the same surface with 400 nm irradiation.[44] The high-temperature side of the CH_3OH TPD peak was depleted preferentially as the laser irradiation time increased. We previously attributed this preferential depletion to the combination of the CH_3OH TPD peak depletion and the shift of the CH_3OH TPD peak toward lower temperature resulting from the hydroxyl groups at bridge bonded oxygen (BBO) sites resulting from CH_3OH dissociation.[44] A very small shoulder also appears on the low-temperature edge of the main TPD peak after 600 s of irradiation, and this shoulder is assigned to $HCOOCH_3$ from photoinduced cross coupling of CH_3O and CH_2O on the surface.[49]

Typical TPD spectra collected at m/z = 31 following 266 nm irradiation are shown in Figure 1B. The evolution of the TPD spectrum with 266 nm irradiation is similar to that with 355 nm irradiation. Given the ratio of photon fluxes at 355 and 266 nm irradiation (1.37:1.00) and the ratio of absorption cross sections at 266 and 355 nm (1.5:1.0), the number of electron−hole pairs created per unit time is expected to be about the same with 266 and 355 nm irradiation. Thus, it is remarkable to see that the CH_3OH depletion after just 5 s irradiation of the 266 nm laser (40 mW) is significantly larger than that after 600 s irradiation of the 355 nm laser (40 mW). This result suggests that CH_3OH photocatalysis at 266 nm is much faster than at 355 nm. Similar to the TPD peak following 355 nm irradiation, the peak following 266 nm irradiation shows a small shoulder on the low-temperature edge, which is again assigned to desorption of the secondary $HCOOCH_3$ product.

In addition to the TPD spectra at m/z = 31, we have collected TPD spectra at m/z = 30 (CH_2O^+) at several different irradiation times with both 355 and 266 nm laser light. Representative TPD spectra are shown in Figure 2A,B. In these TPD spectra, a prominent TPD peak near 265 K can be clearly seen. This peak is assigned to the CH_2O product, which desorbs around 270 K on a clean TiO_2(110) surface.[50] Note here that hydroxyls on BBO sites would reduce the molecular absorption energy on Ti_{5c} sites, as in the case of CH_3OH. With irradiation at a given wavelength (266 and 355 nm), the time scale on which the CH_2O product increases is similar to that of CH_3OH depletion, indicating that the initial main product of photocatalytic CH_3OH dissociation is CH_2O. The photocatalysis of CH_3OH at 400 nm on the same surface also yields CH_2O as the main initial product. Thus, the photocatalytic dissociation of CH_3OH on TiO_2(110) at 355 and 266 nm is assumed to proceed through the same two-step dissociation mechanism that was demonstrated for 400 nm CH_3OH photocatalysis:[44]

$$CH_3OH(Ti_{5c}) \xrightarrow{h\nu} CH_3O(Ti_{5c}) + H_{BBO} \quad (1)$$

$$CH_3O(Ti_{5c}) \xrightarrow{h\nu} CH_2O(Ti_{5c}) + H_{BBO} \quad (2)$$

where H_{BBO} refers to an H atom that is adsorbed on a BBO site. Because the increase in surface temperature during laser irradiation is quite small (only about 5 K), both dissociation steps must be photoinduced and not thermally activated.

CH_2O may be desorbed by light;[49] thus, monitoring the CH_2O product yield is not the best approach to measure the product formation rate, as the CH_2O production rate would not be linked directly with the CH_3OH depletion rate. Another major product from CH_3OH dissociation on TiO_2(110) is atomic hydrogen on the BBO sites, resulting from steps (1) and (2). These products do not desorb by light, but upon heating, two H atoms on BBO rows will combine with an oxygen atom

dx.doi.org/10.1021/ja4114598 | J. Am. Chem. Soc. 2013, 135, 19039−19045

on the BBO row to form a H_2O molecule that desorbs around 500 K, leaving behind an oxygen vacancy (BBOv),[44]

$$2H_{BBO} + BBO \rightarrow H_2O + BBOv \quad (3)$$

Monitoring H-atom production through the desorption of H_2O is the preferred way to measure the product formation rate as CH_3OH undergoes photocatalytic dissociation. TPD spectra at m/z = 18 have therefore been measured at seven irradiation times between 0 and 600 s using 355 nm light and at six irradiation times between 0 and 5 s using 266 nm light. Figure 2C shows three TPD spectra at m/z = 18 after laser irradiation times of 0, 60 s, and 600 s with 355 nm light, and Figure 2D shows three TPD spectra at m/z = 18 after laser irradiation times of 0, 0.5, and 5 s with 266 nm light. With these data, we can determine the formation rate of $2H_{BBO}$ through the H_2O TPD signal and therefore the CH_3OH depletion rate.

The calibrated CH_3OH TPD signal at m/z = 31 (peak at 300 K) and the H_2O TPD signal at m/z = 18 (peak at 500 K) at different irradiation times are plotted in Figure 3. The

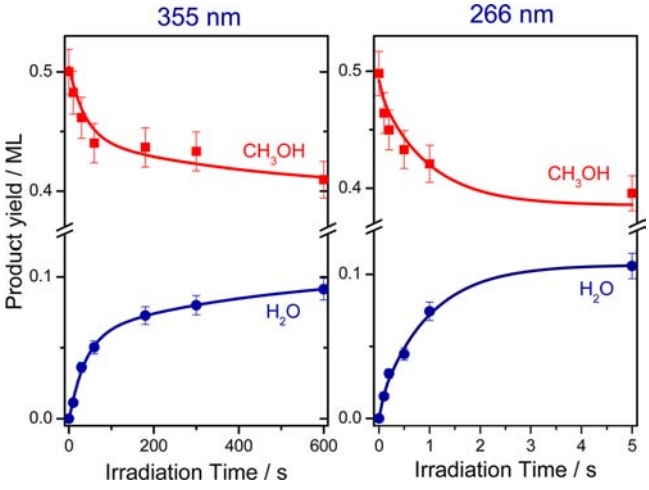

Figure 3. Dependence of CH_3OH and H_2O (from BBO sites) TPD yields on laser irradiation time, at 355 nm (left panel) and 266 nm (right panel). The initially prepared surface was TiO_2(110) with 0.5 ML of adsorbed CH_3OH. The background H_2O TPD signal (t = 0) from CH_3OH dissociation on the BBO vacancy sites has been subtracted from the total H_2O TPD signals. Solid squares and circles are the experimental data (calibrated), while the solid lines are exponential functions that appear to follow the data very well.

background TPD H_2O signal at t = 0 from the spontaneous dissociation of CH_3OH on BBOv has been subtracted from the data. These two plots, corresponding to 255 and 266 nm irradiation, show the correlation between the depletion of the CH_3OH TPD signal and the increase of the H_2O TPD signal, with increasing irradiation time.

DISCUSSION

The results in Figure 3 show clearly that the depletion of the CH_3OH TPD peak and the increase of the H_2O TPD peak are almost exactly anticorrelated at both wavelengths, suggesting that the H_2O peak comes entirely from H atoms on the BBO sites. From the plots of TPD H_2O product yield as a function of irradiation time (Figure 4), we found the rise times at 90% of the asymptotic value to be 280 s for 355 nm and 2.8 s for 266 nm. A more precise determination of the difference in reaction rates at the two wavelengths may be obtained from quantum

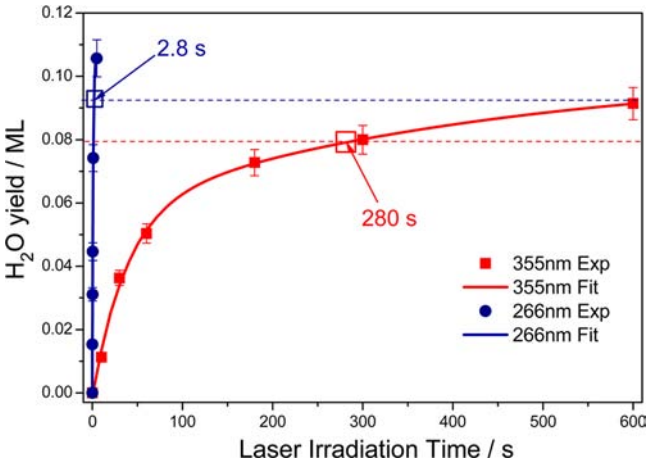

Figure 4. Laser irradiation time dependence of the H_2O (from BBO) TPD yield following 355 nm (left panel) and 266 nm (right panel) irradiation of a 0.5 ML CH_3OH covered TiO_2(110) surface. The solid squares and circles are the experimental data (calibrated), while the solid lines are exponential functions that appear to follow the data very well. The open squares indicate the rise times at 90% of the asymptotic values of the fits for both 355 and 266 nm photocatalysis.

yields. As a result of the accumulation of H atoms on BBO sites during CH_3OH dissociation, as shown in eqs 1 and 2, the quantum yield of the reaction will be much lower for longer irradiation times. The quantum yields were thus calculated from the TPD spectra after short irradiation times where the yield of the H_2O product had a quasi-linear relationship with laser irradiation time. The times chosen for 355 and 266 nm were 60 and 0.5 s, respectively. The resulting quantum yields were 3.3×10^{-6} for 355 nm and 5.5×10^{-4} for 266 nm, suggesting that the initial dissociation rate of CH_3OH at 266 nm is more than 2 orders of magnitude faster than that at 355 nm, in rough agreement with the simple rise-time analysis.

The large difference between the photocatalytic dissociation rates at the two wavelengths is surprising, because it is inconsistent with the prediction from the widely accepted photocatalysis model that charge carriers in TiO_2 rapidly thermalize to their respective band edges, and as a result, the reaction rate should be dependent on the number of electron–hole pairs generated and independent of wavelength. Our experimental result clearly indicates that the energy of the excited electron–hole pairs is also important.

One possible mechanism by which photon energy could influence the dissociation rate would be through dissociative electron attachment (DEA).[24] A 266 nm photon has an energy of 4.67 eV, and the work function of a CH_3OH-covered TiO_2(110) surface is only about 4 eV.[34] Free electrons could thus be produced during irradiation, and these free electrons could induce DEA of CH_3OH.[51] However, the density of electron states near the Fermi level (E_F) of reduced TiO_2(110) surfaces is quite small,[52,53] and the density of free electrons would be very low. Furthermore, DEA of gas-phase CH_3OH is generally observed for electron attachment resonances that lie >6 eV.[51] Thus, DEA by a free electron is expected to make little or no contribution to the photoinduced dissociation of CH_3OH on TiO_2(110).

Electrons excited into the conduction band could also be transferred to unoccupied levels of CH_3OH or CH_3O (e.g., the lowest unoccupied molecular orbital, LUMO), that lie at or below the energy of the photoinduced ("hot") electrons, and

dx.doi.org/10.1021/ja4114598 | J. Am. Chem. Soc. 2013, 135, 19039–19045

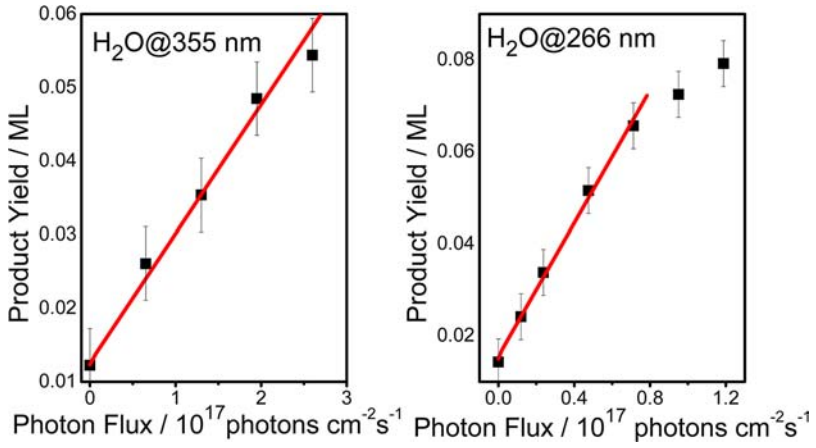

Figure 5. H_2O product yield from 0.5 ML CH_3OH adsorbed $TiO_2(110)$ as a function of photon flux with 355 and 266 nm irradiation. The irradiation times chosen for 355 and 266 nm are 60 and 2 s, respectively. The surface temperature (~110 K) was nearly unchanged during irradiation. These data were collected with a new sample (i.e., a different sample than was used in the other experiments). Although the sample was prepared in the same way at the previous sample, the product yields from the new sample were lower.

then anion excited states of the adsorbate which are formed by electron transfer at the $TiO_2(110)$ interface could result in dissociation of the adsorbate. This dissociation mechanism might seem unlikely, because the LUMO of the CH_3OH molecule is calculated to be +0.69 eV,[54] making it higher than the vacuum level. However, when molecules adsorb on a surface, the LUMO generally shifts ~1−2 eV lower in energy.[55] Assuming a width of 1 eV (based on the observed full width at half-maximum of the low-energy resonance for electron attachment to gas-phase CH_3OH),[51] it would be possible for a conduction-band electron to transfer to the LUMO of CH_3OH.

The transfer of a hole to the CH_3OH might be another mechanism for dissociation. Based on ultraviolet photoelectron spectroscopy data,[21,25,56] the highest occupied molecular orbital (HOMO) of CH_3OH adsorbed on $TiO_2(110)$ relative to the valence band maximum (VBM) is reported to be ~2 eV. Previous studies show that the photocatalytic dissociation of CH_3OH on $TiO_2(110)$ can occur even with 400 nm irradiation.[40,44] There will be a large energy mismatch between photogenerated holes in the valence band by 400 nm (3.1 eV) irradiation and the electronic states of CH_3OH. Thus, hole transfer to CH_3OH is unlikely.

Another possible explanation for photoinduced dissociation of CH_3OH on $TiO_2(110)$ is that the dissociation occurs on the ground electronic state surface. In this case, the initially formed electrons would thermalize to the conduction band minimum (CBM) within hundreds of femtoseconds[15] and then recombine with the holes, in a process that is analogous to internal conversion in the gas phase.[57] As a result, the photon energy would be fully converted to local phonon energy in a short time. Through vibrational redistribution between the highly excited phonon modes and the vibrational modes of CH_3OH or CH_3O in a localized area, the adsorbate could gain sufficient energy to dissociate before the phonons dissipated their energy into the bulk. Sufficient energy for dissociation on the ground state might become available through a single-photon event, as implied above, or through a multiphoton process involving the excitation of many phonons. The efficiency of this "ladder-climbing" process would be expected to be nonlinear with photon flux. We thus investigated the yield of H_2O as a function of photon flux at 266 and 355 nm (see Figure 5). Within experimental error, the H_2O yield at 355 nm is linear with photon flux from 0 to 2.6×10^{17} photons cm^{-2} s^{-1}. The H_2O yield at 266 nm is approximately linear up to about 7.1×10^{16} photons cm^{-2} s^{-1}, and then it appears to begin to saturate as the power is raised to 1.2×10^{17} photons cm^{-2} s^{-1}. With both irradiation wavelengths, there is no evidence for the exponential increase in yield that would be expected for a multiphoton, or ladder-climbing, process. If a dissociation step proceeds on the ground electronic state potential energy surface, then it may be a single-photon process where the photon energy is rapidly converted to high phonon excitation that can, in turn, rapidly couple to the reaction coordinate in the adsorbate (CH_3OH or CH_3O).

The apparent saturation in the H_2O yield with high photon fluxes of 266 nm light might be the result of the photoejection of H_{BBO} atoms, which is possible at this short wavelength (see Figure S2). The loss of H_{BBO} atoms would reduce the availability of hydroxyls at BBO sites for the production of H_2O. The fact that the saturation is very mild at the laser powers used suggests that the ejection of H_{BBO} plays a minor role and should have no bearing on the conclusion about the strong photon-energy dependence of the dissociation yield of CH_3OH on $TiO_2(110)$.

■ CONCLUSION

In summary, our wavelength-dependent TPD investigation provides evidence that the relative quantum yield of H_{BBO} from the photoinduced decomposition of CH_3OH on $TiO_2(110)$ at 266 nm is more than 100 times higher than that at 355 nm, indicating that the reaction is strongly dependent on the irradiation wavelength. This result contradicts a widely accepted model of photocatalysis on $TiO_2(110)$, which assumes that charge carriers in TiO_2 rapidly thermalize to their respective band edges via strong coupling with phonon modes and reaction is thus only dependent on the number of electron−hole pairs created during photoexcitation. Plausible explanations for the wavelength-dependent rate are reaction on the ground-state potential energy surface or transfer of a conduction band electron to the LUMO of CH_3OH or CH_2O. The importance of the electron−hole pair energy demonstrated in this work calls for the development of a more sophisticated surface photocatalysis model that incorporates the

dx.doi.org/10.1021/ja4114598 | J. Am. Chem. Soc. 2013, 135, 19039−19045

effect of photon energy. Such development is expected to enhance our understanding of fundamental processes in photocatalysis and guide the development of more efficient photocatalysts in the future.

■ ASSOCIATED CONTENT

Supporting Information

Additional information as noted in the text. This material is available free of charge via the Internet at http://pubs.acs.org.

■ AUTHOR INFORMATION

Corresponding Authors

guoqing@dicp.ac.cn
tminton@montana.edu
xmyang@dicp.ac.cn

Present Address

[⊥]Also with School of Physics and Optoelectric Engineering, Dalian University of Technology, Dalian, Liaoning 116023, China

Author Contributions

[∥]These authors made similar contributions to this work.

Notes

The authors declare no competing financial interest.

■ ACKNOWLEDGMENTS

This work was supported by the Chinese Academy of Sciences, National Science Foundation of China, and the Chinese Ministry of Science and Technology. We also wish to thank Prof. Hongjun Fan for many helpful discussions and theoretical calculations during the course of this work.

■ REFERENCES

(1) Fujishima, A.; Honda, K. *Nature* **1972**, *238*, 37−38.
(2) Linsebigler, A. L.; Lu, G.; Yates, J. T. *Chem. Rev.* **1995**, *95*, 735−758.
(3) Fujishima, A.; Zhang, X.; Tryk, D. A. *Surf. Sci. Rep.* **2008**, *63*, 515−582.
(4) Gaga, U. I.; Abdullah, A. H. *J. Photochem. Photobiol., C* **2008**, *9*, 1−12.
(5) Hoffmann, M. R.; Martin, S. T.; Choi, W. Y.; Bahnemann, D. W. *Chem. Rev.* **1995**, *95*, 69−96.
(6) Thompson, T. L.; Yates, J. T., Jr. *Chem. Rev.* **2006**, *106*, 4428−4453.
(7) Henderson, M. A.; Otero-Tapia, S.; Castro, M. E. *Faraday Discuss.* **1999**, *114*, 313−319.
(8) Gong, X.-Q.; Selloni, A.; Dulub, O.; Jacobson, P.; Diebold, U. *J. Am. Chem. Soc.* **2008**, *130*, 370−381.
(9) Pang, C. L.; Lindsay, R.; Thornton, G. *Chem. Soc. Rev.* **2008**, *37*, 2328−2353.
(10) Fujishima, A.; Zhang, X.; Tryk, D. *Surf. Sci. Rep.* **2008**, *63*, 515−582.
(11) Diebold, U. *Surf. Sci. Rep.* **2003**, *48*, 53−229.
(12) Enache, D. I.; Edwards, J. K.; Landon, P.; Solsona-Espriu, S.; Carley, A. F.; Herzing, A. A.; Watanabe, M.; Kiely, C. J.; Knight, D. W.; Hutchings, G. J. *Science* **2006**, *311*, 362−365.
(13) Khan, S. M.; Al-Shahry, M.; Ingler, W. B., Jr. *Science* **2002**, *297*, 2243−2245.
(14) Green, I. X.; Wang, W.; Neurock, M.; Yates, J. T., Jr. *Science* **2012**, *333*, 736−739.
(15) Henderson, M. A. *Surf. Sci. Rep.* **2011**, *66*, 185−297.
(16) Gundlach, L.; Felber, S.; Storck, W.; Galoppini, E.; Wei, Q.; Willig, F. *Res. Chem. Intermed.* **2005**, *31*, 39−46.
(17) Gundlach, L.; Ernstorfer, R.; Willig, F. *Phys. Rev. B* **2006**, *74*, 035324.
(18) Nilius, N.; Ernst, N.; Freund, H.-J. *Chem. Phys. Lett.* **2001**, *349*, 351−357.
(19) Yamada, Y.; Kanemitsu, Y. *Phys. Rev. B* **2010**, *82*, 113103.
(20) Yamada, Y.; Kanemitsu, Y. *Phys. Status Solidi C* **2011**, *8*, 104−107.
(21) Sporleder, D.; Wilson, D. P.; White, M. G. *J. Phys. Chem. C* **2009**, *113*, 13180−13191.
(22) Diwald, O.; Thompson, T. L.; Goralski, Ed. G.; Walck, S. D.; Yates, J. T., Jr. *J. Phys. Chem. B* **2004**, *108*, 52−57.
(23) Brusa, M. A.; Grela, M. A. *J. Phys. Chem. B* **2005**, *109*, 1914−1918.
(24) Kim, S. H.; Stair, P. C.; Weitz, E. *J. Chem. Phys.* **1998**, *108*, 5080−5088.
(25) Grela, M. A.; Colussi, A. J. *J. Phys. Chem. B* **1999**, *103*, 2614−2619.
(26) Stafford, U.; Gray, K. A.; Kamat, P. V. *J. Catal.* **1997**, *167*, 25−32.
(27) Kawai, T.; Sakata, T. *J. Chem. Soc. Chem. Commun.* **1980**, 694−695.
(28) Henderson, M. A.; Otero-Tapia, S.; Castro, M. E. *Surf. Sci.* **1998**, *412/413*, 252−272.
(29) Farfan-Arribas, E.; Madix, R. J. *Surf. Sci.* **2003**, *544*, 241−260.
(30) Zhang, Z. R.; Bondarchuk, O.; White, J. M.; Kay, B. D.; Dohnálek, Z. *J. Am. Chem. Soc.* **2006**, *128*, 4198−4199.
(31) Sanchez de Armas, R.; Oviedo, J.; San Miguel, M. A.; Sanz, J. F. *J. Phys. Chem. C* **2007**, *111*, 10023−10028.
(32) Oviedo, J.; Sanchez de Armas, R.; San Miguel, M. A.; Sanz, J. F. *J. Phys. Chem. C* **2008**, *112*, 17737−17740.
(33) Farfan-Arribas, E.; Madix, R. J. *J. Phys. Chem. B* **2002**, *106*, 10680−10692.
(34) Onda, K.; Li, B.; Zhao, J.; Petek, H. *Surf. Sci.* **2005**, *593*, 32−37.
(35) Wang, L.-Q.; Ferris, K. F.; Winokur, J. P.; Shultz, A. N.; Baer, D. R.; Engelhard, M. H. *J. Vac. Sci. Technol., A* **1998**, *16*, 3034−3040.
(36) Sanchez, V. M.; Cojulun, J. A.; Scherlis, D. A. *J. Phys. Chem. C* **2010**, *114*, 11522−11526.
(37) Martinez, U.; Vilhelmsen, L. B.; Kristoffersen, H. H.; Stausholm-Moller, J.; Hammer, B. *Phys. Rev. B* **2011**, *84*, 205434.
(38) Zhao, J.; Yang, J. L.; Petek, H. *Phys. Rev. B* **2009**, *80*, 235416.
(39) Wong, G. S.; Kragten, D. D.; Vohs, J. M. *J. Phys. Chem. B* **2001**, *105*, 1366−1373.
(40) Zhou, C.; Ren, Z.; Tan, S.; Ma, Z.; Mao, X.; Dai, D.; Fan, H.; Yang, X.; LaRue, J.; Cooper, R.; Wodtke, A. M.; Wang, Z.; Li, Z.; Wang, B.; Yang, J.; Hou, J. *Chem. Sci.* **2010**, *1*, 575−580.
(41) Zhou, C. Y.; Ma, Z. B.; Ren, Z. F.; Mao, X. C.; Dai, D. X.; Yang, X. M. *Chem. Sci.* **2011**, *2*, 1980−1983.
(42) Shen, M.; Henderson, M. A. *J. Phys. Chem. Lett.* **2011**, *2*, 2707−2710.
(43) Ahmed, A. Y.; Kandiel, T. A.; Oekermann, T.; Bahnemann, D. *J. Phys. Chem. Lett.* **2011**, *2*, 2461−2465.
(44) Guo, Q.; Xu, C.; Ren, Z.; Yang, W.; Ma, Z.; Dai, D.; Fan, H.; Minton, T. K.; Yang, X. *J. Am. Chem. Soc.* **2012**, *134*, 13366−13373.
(45) Shen, M.; Henderson, M. A. *J. Phys. Chem. C* **2012**, *116*, 18788−18795.
(46) Shen, M.; Acharya, D. P.; Dohnálek, Z.; Henderson, M. A. *J. Phys. Chem. C* **2012**, *116*, 25465−25469.
(47) Ren, Z.; Guo, Q.; Xu, C.; Yang, W.; Xiao, C.; Dai, D.; Yang, X. *Chin. J. Chem. Phys.* **2012**, *5*, 507−512.
(48) Zehr, R. T.; Henderson, M. A. *Surf. Sci.* **2008**, *602*, 1507−1516.
(49) Guo, Q.; Xu, C.; Yang, W.; Ren, Z.; Ma, Z.; Dai, D.; Minton, T. K.; Yang, X. *J. Phys. Chem. C* **2013**, *117*, 5293−5300.
(50) Lu, G.; Linsebigler, A.; Yates, J. T., Jr. *J. Phys. Chem.* **1994**, *98*, 11733−11738.
(51) Ibănescu, B. C.; Allan, M. *Phys. Chem. Chem. Phys.* **2008**, *10*, 5232−5237.
(52) Henderson, M. A.; Epling, W. S.; Perkins, C. L.; Peden, C. H. F.; Diebold, U. J. *Phys. Chem. B* **1999**, *103*, 5328−5337.
(53) Kurtz, R. L.; Stockbauer, R.; Madey, T. E.; Roman, E.; Desegovia, J. L. *Surf. Sci.* **1989**, *218*, 178−200.

(54) The LUMO of the CH_3OH molecule is calculated to be +0.69 eV by a Hartree−Fock approach using Gaussian 09. (Geometry optimization: ccsd/cc-pVTZ basis set; single point energy: ccsd(t)/aug-cc-pVTZ basis set.)
(55) Feulner, P.; Menzel, D. Laser Spectroscopy and Photo-Chemistry on Metal Surfaces, Part II. In *Advanced Series in Physical Chemistry*; Hai-Lung Dai, W. H., Ed.; World Scientific: Singapore, 1995; Vol. 5; p 627.
(56) Wang, L.-X.; Ferris, K. F.; Winokur, J. P.; Shultz, A. N.; Baer, D. R.; Engelhard, M. H. *J. Vac. Sci. Technol., A* **1998**, *16*, 3034.
(57) Felker, P. M.; Zewail, A. H. *J. Chem. Phys.* **1985**, *82*, 2961−2974.